Tensile flow stress of non-oriented Fe-3.3%Si steel at a wide range of moderate temperatures

Mei Rui-bin[1,2], Bao Li[2], Li Guang-lin[3], Zhang Jie[1], Zhang Xin[1,2], Qi Xi-wei[2]
1. *State Key Laboratory of Rolling and Automation, Northeastern University, Shenyang 110819, Liaoning, China；*
2. Northeastern University at Qinhuangdao, Northeastern University, Qinhuangdao 066004, Hebei, China；
3. Ironmaking plant of Shougang Qian’an iron and steel Co Ltd, Qian’an 064404, Hebei, China
E-mail: meirb1999@gmail.com

Abstract: The flow stress behavior of hot-rolled Fe-3.3%Si steel was studied through single-pass warm tensile experiments within the temperature range of 250 to 700 °C and strain rate range of 0.001 s^{-1} to 0.1 s^{-1}. The peak stress decreased linearly, but the elongation increased exponentially, with an increase in temperature. Work hardening behavior was obvious, and the non-uniform plastic deformation stage was shorter at lower temperatures, and accordingly the grains were elongated. A novel method was proposed to describe the tensile flow stress of Fe-3.3%Si steel at wide moderate temperatures, and the flow behavior of Fe-3.3%Si was described as the function of temperature, strain and strain rate. The capability of the model to predict tensile flow stress was investigated and the predicted results were in good agreement with measured values. Therefore, the model is reliable and helpful for the optimization of deformation parameters in warm processing.
Keywords: tension; silicon steel; flow stress; moderate temperature.

1. Introduction

As an important soft magnetic alloy, non-oriented silicon steel is widely applied in the power, electronic, and military industries. Many researchers have studied the improvement of microstructural and magnetic properties of non-oriented steel by varying chemical composition, heating and cooling technologies, rolling parameters, and annealing processes [1-4]. Fe-3.3% Si steel is a high grade cold-rolled non-oriented electrical steel that exhibits obvious brittleness and poor cold-working ability [5]. Below the recrystallization temperature, recovery in metal forming occurs through an increase in the deformation temperature, which is helpful for the improvement of plastic deformation. For this reason, warm rolling is usually applied to silicon steel to improve its microstructural and magnetic properties [6-8]. The influence of the rolling parameters and deformation temperature on the texture and microstructure of non-oriented Fe-2.1%Si steel during warm rolling processing was previously investigated by Zhang [9]. They found that the deformation texture changed from a shear texture at the surface to a planar texture at the center. Furthermore, shear banding occurred in the grains and the grains were elongated along the rolling direction at rolling temperatures of approximately 200-500 °C. The deformation behavior at a moderate temperature is an important factor in the technological optimization of rolling processes, including cold and hot rolling. Additionally, in order to employ more advanced modeling techniques such as finite element analysis and calculation of deformation loads, the constitutive behavior during deformation regimes must be elucidated.

The ductility of the magnetic material of Fe with 6.5 wt.% Si was previously investigated and its constitutive equation for warm deformation established by Li et al. [10]. Intergranular fractures could be transformed into quasicleavage fractures, which greatly improved the ductility of warm-rolled sheets at high rolling temperatures. The Johnson-Cook (JC) model was modified and employed by Zhang et al. [11] to predict the flow behavior of advanced high-strength steel at a wide range of temperatures from 298 to 1073K. The accuracy of the modified JC model was further verified, and the predicted flow stress was shown to be in good agreement with experimental results. Li et al. [12] investigated the warm deformation behavior of quenched 0.45C steel and established the corresponding constitutive equations.

Currently, despite many studies reporting on the improvement of microstructural and magnetic properties [13-15], few studies exist on the warm deformation behavior and constitutive equations of Fe-Si steel. In the present

work, the warm deformation behavior of a hot-rolled Fe-3.3%Si steel strip was therefore investigated using warm tensile experiments at a temperature range of approximately 250-700 °C and strain rate range of approximately 0.001-0.1 s^{-1}. A new model was then proposed to express the change in flow stress during hardening and elongation. Simultaneously, new hardening index functions, which are sensitive to temperature and strain rate, were proposed in the developed constitutive model. This study is of great importance for the study and optimization of the parameters of silicon steel during warm deformation processes as well as rolling.

2. Materials and Methods

The raw material in this study was a hot-rolled Fe-3.3%Si steel strip from a plant in China with chemical composition as shown in Table 1.

Table 1 Chemical composition of Fe-3.3%Si steel (wt.%).

Element	C	Fe	Si	Mn	Cu	S	Cr	Al
Contents	0.0015	96.3	3.28	0.099	0.021	0.0097	0.012	0.042

The thickness of the original sample was 2.5 mm, and standard tension specimens were cut with a total length of 200 mm, parallel section length of 50 mm, and gauge length of 30 mm, as shown in Fig. 1. A single-pass warm tensile test was carried out using an Inspekt Table 100 kN (Hegewald&Peschke,Germany) with samples at strain rates of 0.001, 0.01, and 0.1 s^{-1}, and deformation temperatures of 250 °C, 400 °C, 550 °C, and 700 °C. Samples were first heated to their deformation temperature at 20 °C/min, and then the heat preservation time was 10 minutes in order to obtain a uniform temperature. The temperature was kept stable during all tensile processes. The oxide layer on the fracture surface of specimens was subsequently removed using ultrasonic equipment, and their fracture morphologies examined using a SUPRA 55 SEM (Zeiss,Germany). Furthermore, the microstructure in the tensile direction and X-ray diffraction (XRD) patterns were examined by a DMI5000m (Leica,Germany) and Smartlab 9 (Rigaku, Japan). The used corrosion mixture was a mixture of 95 % alcohol and 5 % H_2NO_3.

Figure 1. Part of the original tension samples.

3. Results and Discussions

3.1. Flow Stress

The true stress-strain curves at different strain rates and temperatures are shown in Fig. 2. As can be seen, an increase in deformation temperature resulted in a significant decrease in peak stress and increase in elongation. Work hardening obviously occurred during metal forming at a deformation temperature of 250 °C, with a shorter non-uniform plastic deformation stage. When the deformation temperatures were 250 °C and 400 °C, samples rapidly underwent tensile breaking upon experiencing a stress greater than their peak stress, resulting in the obvious load drop. When the deformation temperature was 550 °C, on the other hand, flow stress increased to peak value first due to the main effect of work hardening, after which the deformation distortion provided the driving force for dynamic recrystallization softening during continuous deformation, resulting in a subsequent slow decrease in flow stress. Increasing the strain rate had a smaller effect on the increase in stress at deformation temperatures of 250 °C and 400 °C, because few slip systems exist at lower temperatures.

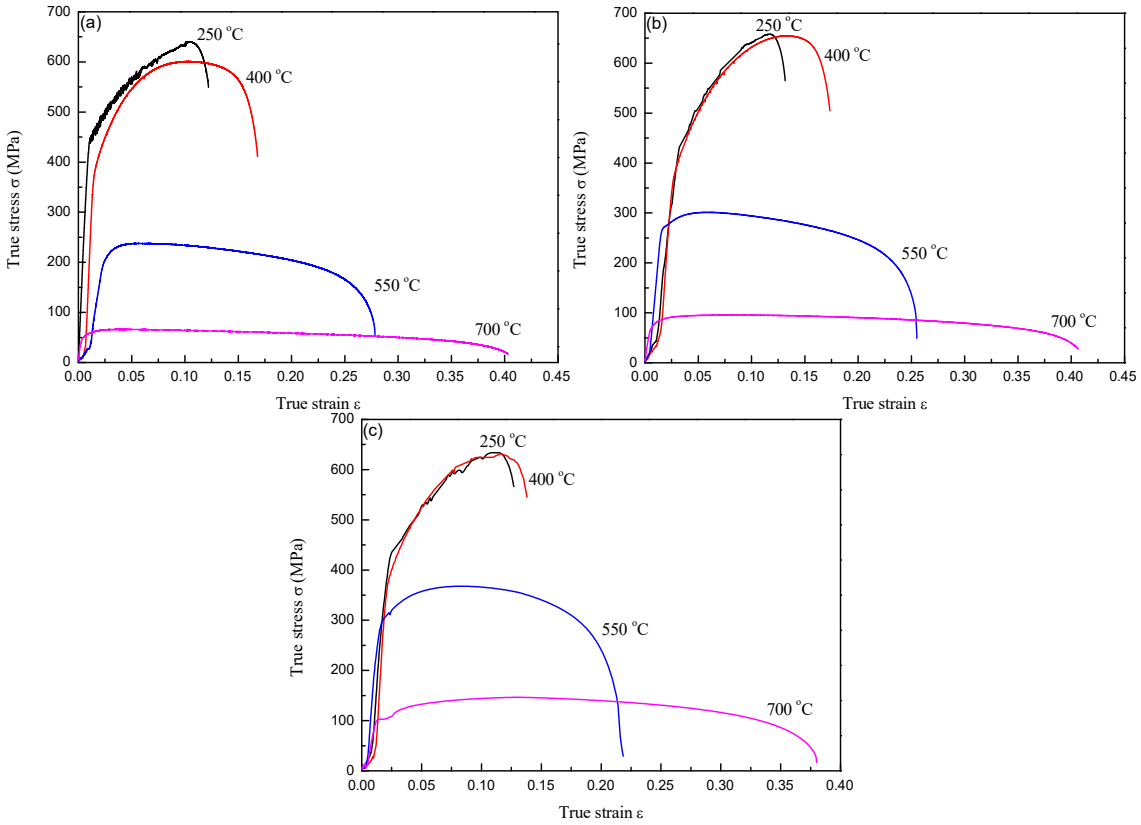

Figure 2. True stress-strain curves of Fe-3.3%Si steel during moderate temperature tensile testing at different strain rates: (a) 0.001 s^{-1}; (b) 0.01 s^{-1}; (c) 0.1 s^{-1}.

The measured peak stress and elongation values of Fe-3.3%Si steel strips are shown in Fig. 3. The peak stress decrease approximated a linear function, especially within the deformation temperature range from 400 °C to 700 °C. However, elongation increased exponentially with the increase in temperature, indicating that the increase in temperature is beneficial for plastic deformation. The effects of the strain rate on peak stress and elongation became more significant at higher temperatures than at 250 °C. The reason for this might be that the slip system is not active at lower deformation temperatures. With an increase in strain rate, the dislocation movement was hindered from forming micro-cracks, so that peak stress increased, but elongation obviously decreased. Dynamic softening occurs more easily at higher deformation temperatures, which leads to a lower peak stress and higher elongation. Furthermore, lower strain rates allow sufficient time for dynamic softening processes to occur, especially at higher temperatures, and accordingly the tensile strength decreases and elongation increases significantly.

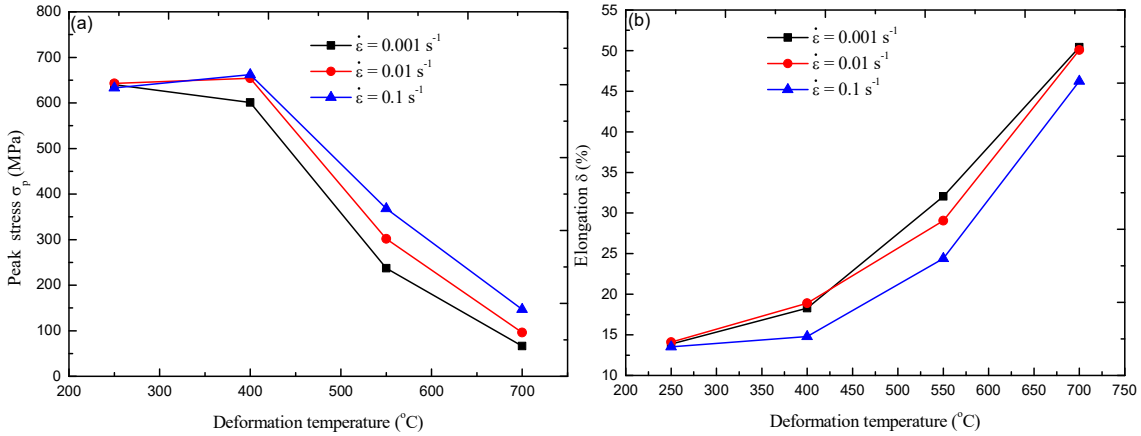

Figure 3. Peak stress and elongation of Fe-3.3%Si steel: (a) peak stress; (b) elongation.

3.2 Modeling of flow stress

A constitutive relation is generally used to describe the plastic flow properties of metals and alloys, which are only correlated with strain in case of cold deformation, but additionally with strain rate and deformation temperature in case of hot deformation. Since 700 °C is less than the conventional hot deformation temperature

for Fe-Si steel, hardening is the main influencing factor at moderate temperatures. On the basis of cold deformation behavior, strain was first considered for the constitutive equation and expressed as:

$$\sigma = A\varepsilon^n \tag{1}$$

where A is a coefficient that can be obtained from the line slope of the σ-ε^n plot; n is the hardening index, of which the value is the slope of the $\ln(\sigma)$-$\ln(\varepsilon)$ plot found through transformation of the natural logarithm of equation (1) into $\ln(\sigma)=\ln(A)-n\cdot\ln(\varepsilon)$.

The relationship between $\ln(\sigma)$ and $\ln(\varepsilon)$ at different temperatures and strain rates is shown in Fig. 4, with true stresses ranging from yield to peak values. From this figure, it is obvious that the hardening processes became shorter at higher temperatures and lower strain rates. The main reason for this is the easier and more complete dynamic recovery or recrystallization generated during tension. In addition, the hardening index of the material was approximately higher at higher temperatures and lower strain rates, with the influence of the temperature on the hardening index more obvious compared to that of the strain rate. As an example, the average hardening indices were about 0.26 and 0.28 at temperatures of 250 °C and 400 °C, respectively, but only 0.098 and 0.097 at temperatures of 550 °C and 700 °C, respectively. When the deformation temperatures were 250 °C and 400 °C, the corresponding hardening indices at a strain rate of 0.1 s^{-1} were significantly lower than those at 0.01 s^{-1}, possibly because the thermal effect is relatively more significant at higher deformation speeds and lower temperatures.

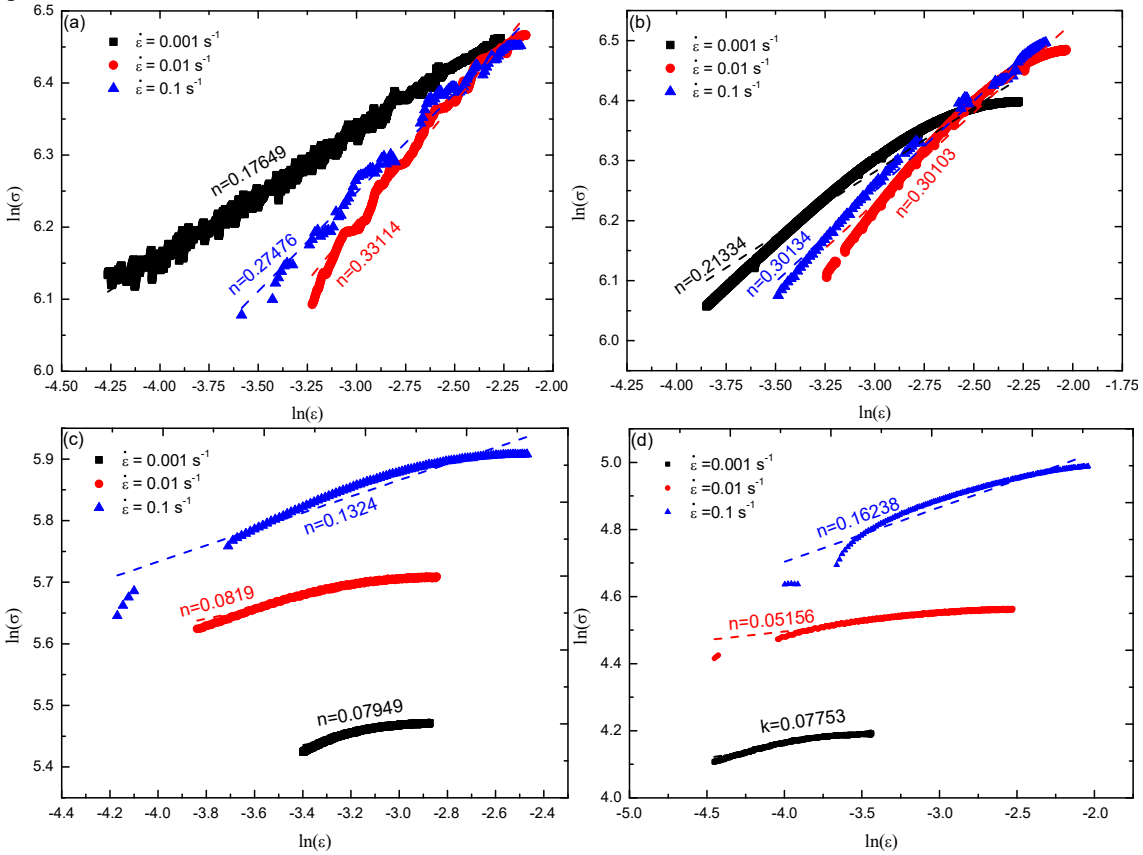

Figure 4. The relationship between ln(σ) and ln(ε) values at varying temperatures and strain rates: (a) 250 °C; (b) 400 °C; (c) 550 °C; (d) 700 °C.

As both the deformation temperature and strain rate were found to have an effect on the hardening index, the values at a strain rate of 0.01 s^{-1} were used as the reference conditions to model the following equation:

$$\frac{n}{n_{0.01}} = \left(\frac{\dot{\varepsilon}}{0.01}\right)^B \tag{2}$$

where B equals the average slope of the $\ln\left(n/n_{0.01}\right)-\ln(\dot{\varepsilon}/0.01)$ plot shown in Fig. 5, with a value of 0.109. The value of $n_{0.01}$ is the hardening index at the given strain rate of 0.01 s^{-1} at different deformation temperatures. According to the fitting results, $n_{0.01}$ can be expressed as:

$$n_{0.01} = 0.527 - 7.05\times10^{-4}\cdot T \tag{3}$$

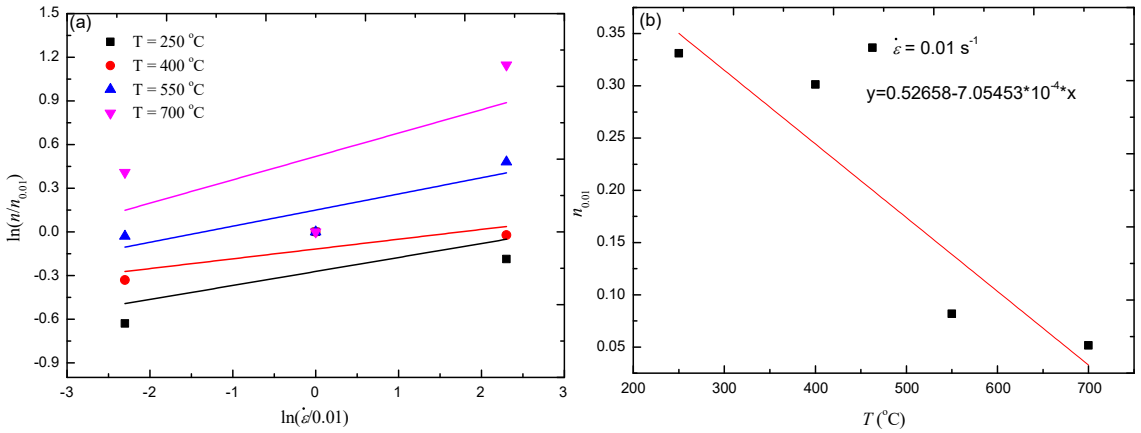

Figure 5. The relationship between: (a) $\ln(n/n_{0.01})$ and $\ln(\dot{\varepsilon}/0.01)$ at different temperatures; (b) $n_{0.01}$ and T.

When the value of n is substituted into equation (1) for different temperatures and strain rates, the values for A are the slopes of the $\sigma-\dot{\varepsilon}^n$ plots shown in Fig. 6. With an increase in temperature and decrease in strain rate, the value of A decreased significantly. However, the deformation temperature had a greater effect than the strain rate. Using the same method for obtaining n, A can be described by equation (4), with plots shown in Fig. 7.

$$A=(2184.32-2.994\cdot T)\cdot\left(\frac{\dot{\varepsilon}}{0.01}\right)^{0.1121} \tag{4}$$

According to equations (1) to (4), the constitutive equation for non-oriented Fe-3.3%Si steel can then be written as:

$$\sigma=(2184.32-2.994\cdot T)\cdot\left(\frac{\dot{\varepsilon}}{0.01}\right)^{0.1121}\cdot\varepsilon^{(0.527-7.055\times10^{-4}\cdot T)\left(\frac{\dot{\varepsilon}}{\dot{\varepsilon}_{0.01}}\right)^{0.109}} \tag{5}$$

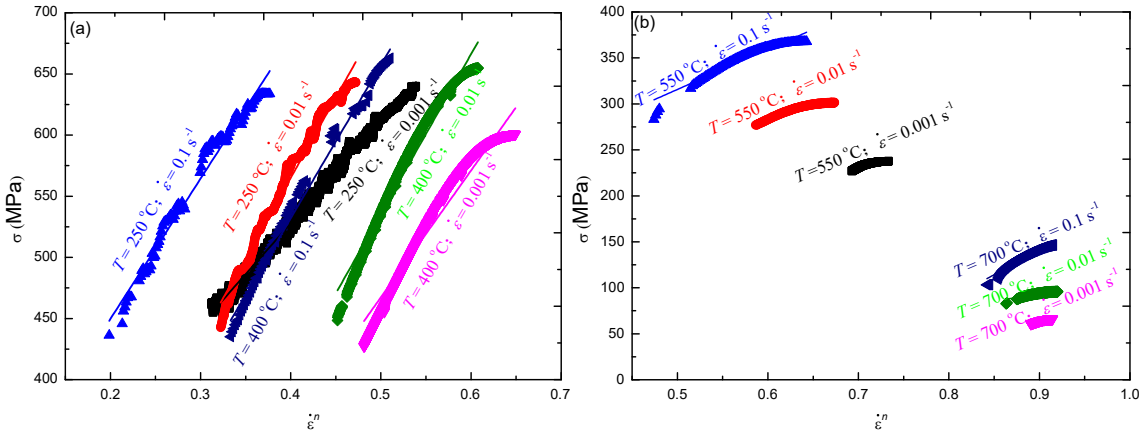

Figure 6. The relationship between σ and $\dot{\varepsilon}^n$ at different temperatures and strain rates.

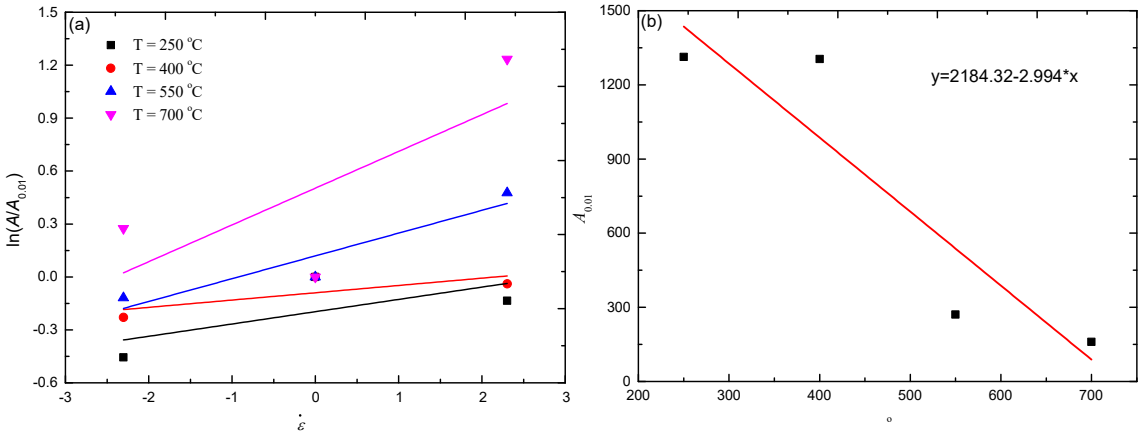

Figure 7. The relationship between: (a) $\ln(A/A_0)$ and $\ln(\dot{\varepsilon}/0.01)$ at different temperatures; (b) $A_{0.01}$ and T.

The performance of the derived constitutive models was further investigated by statistical analysis of the relative error through comparing the predicted results with experimental data. The relative errors were calculated as below [16]:

$$RE_i = \frac{|E_i - P_i|}{E_i} \times 100\% \tag{6}$$

where E_i and P_i are the experimental and predicted flow stresses, respectively.

The predicted relative errors under different conditions are shown in Fig. 8, clearly showing that the predicted flow stresses in the hardening process were in good agreement with the experimental data. The model had a higher predicted precision at a strain rate of 0.01 s^{-1} than at other strain rates. Almost all the predicted relative errors were less than 10 % under conditions of temperature and strain rate of 250 °C and 0.01 s^{-1}, 400 °C and 0.1 s^{-1}, and 700 °C and 0.001 s^{-1}. The model had a lower predicted precision at a temperature of 550 °C. As both the wide temperature and strain rate ranges need to be taken into account, it is difficult to formulate a model with a higher predicted precision. As an example, the relative error was less than 5 % for 98.1 % of results at the temperature of 250 °C and strain rate of 0.01 s^{-1}, but at the temperature of 550 °C and strain rate of 0.001 s^{-1}, the percentage of predicted results with a relative error of more than 20 % was about 88 %. In fact, from the above figures and equations, it was found that the proposed and employed model would have a higher predicted precision if the 550 °C and 700 °C deformation temperatures had not been considered, because the dynamic recrystallization generated above 550 °C resulted in higher errors of n and A. On the whole, the maximum value for the predicted relative error was about 24.87 %, and the proposed and employed constitutive equations were reliable.

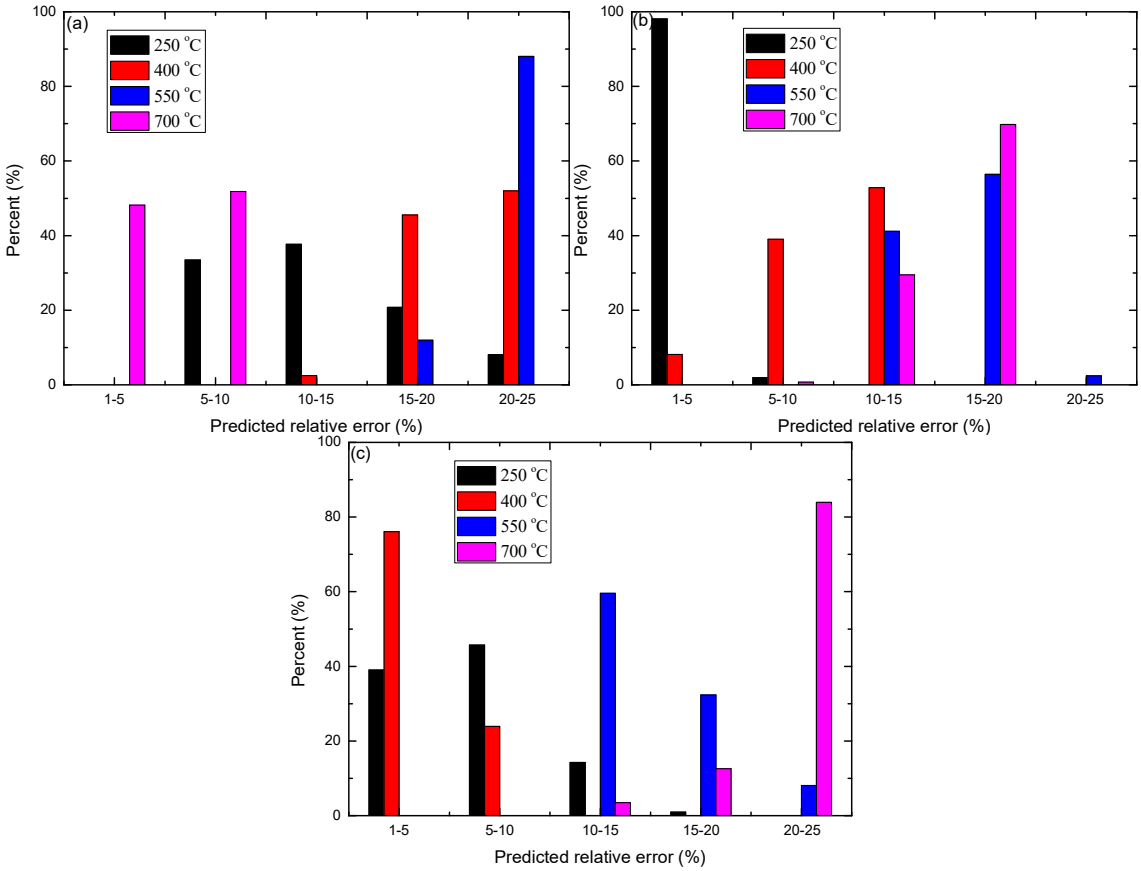

Figure 8. Predicted relative error distribution at different conditions: (a) $\dot{\varepsilon} = 0.001$; (b) $\dot{\varepsilon} = 0.01$; (c) $\dot{\varepsilon} = 0.1$.

4. Conclusions

Hot-rolled non-oriented Fe-3.3%Si steel was studied using tensile testing in the temperature range of 200-700 °C and strain rate range of 0.001-0.1 s^{-1}. Peak stress decreased linearly, but elongation increased exponentially with an increase in deformation temperature. Work hardening behavior obviously occurred and the non-uniform plastic deformation stage was shortened at lower temperatures. The hardening processes of non-oriented Fe-3.3%Si steel were described as a function of the deformation temperature and strain rate. The

predicted results by the proposed model were in good agreement with the measured values, and the models were shown to be reliable. The following equations describe the proposed models for hardening processes:

$$\sigma = (2184.32 - 2.994 \cdot T) \cdot \left(\frac{\dot{\varepsilon}}{0.01}\right)^{0.1121} \cdot \varepsilon^{(0.527 - 7.055\times10^{-4} \cdot T)\left(\frac{\dot{\varepsilon}}{\dot{\varepsilon}_{0.01}}\right)^{0.109}}$$

5. Acknowledgments

The authors gratefully acknowledge financial support from the Natural Science Foundation-Steel and Iron Foundation of Hebei Province (No. E2014501114), the Science and Technological Youth Foundation of Hebei Higher (No. 20132007), as well as the Doctoral Scientific Research Foundation of Liaoning Province (No. 20170520314).

6. References

[1] Zhang W K, Mao W M, Wang Y D, et al. Influence of Hot Rolling Parameters on Microstructure and Magnetic Properties of Non-oriented Electrical Steel. Iron and Steel, 2006, 41(4):77-81.
[2] Yue E B, Li N. Effect of Rare Earth Cerium on the Magnetic Properties of 2.9%Si Non-Oriented Electrical Steels. Iron and Steel, 2014, 49(1): 65-70.
[3] de Dafe S S F, Paolinelli S D, Cota A B. Influence of thermo-mechanical processing on shear bands formation and magnetic properties of a 3%Si non-oriented electrical steel. J. Magn. Magn. Mater., 2011, 323: 3234-3238.
[4] Liu H T, Liu Z Y, Cao G M, et al. Microstructure and texture evolution of strip casting 3wt% Si non-oriented silicon steel with columnar structure. J. Magn. Magn. Mater., 2011, 323: 2648-2651.
[5] Rodrigues M F, da Cunha M A, Paolinelli S D, et al. Texture and magnetic properties improvement of a 3% Si non-oriented electrical steel by Sb addition. J. Magn. Magn. Mater., 2013, 331: 24-27.
[6] Nippon Kokan Kabushiki Kaisha, Sadakazu Masuda, Fumio Fujita, et al. Warm rolling method for high silicon steel strip：US, 0483809 [P/OL]. 1990-07-03.
[7] Liang Y J, Lin J P, Ye F, et al. Effect of Heat Treatment on Microstructure and Properties of Heavily Cold Rolled Fe-6.5 wt% Si Alloy Sheet. Met. Funct. Mater., 2010, 17(2): 43-47.
[8] Liu H T, Liu Z Y, Sun Y, et al. Development of λ-fiber recrystallization texture and magnetic property in Fe–6.5wt% Si thin sheet produced by strip casting and warm rolling method. Mater. Lett., 2013, 91:150-153.
[9] Zhang G P. Influence of rolling gap geometry and temperature on the textures and microstructure of non-oriented electrical steel. Chinese Master's Theses Full-text Database: Engineering Science and Technology I, 2011, S1: 1-59.
[10] Li C S, Cai G J, Cai B, et al. Impact of rolling temperature on microstructure, ordered phases, and ductility in Fe-6.5 wt% Si magnetic material [J]. J. Mater. Res., 2016, 31(19):1-12.
[11] Zhang Q, Qiang C, Zhang X. A Modified Johnson-Cook Model for Advanced High-Strength Steels over a Wide Range of Temperatures. J. Mater. Eng. Perform., 2014, 23(12):4336-4341.
[12] Li Q, Wang T S, Jing T F, et al. Warm deformation behavior of quenched medium carbon steel and its effect on microstructure and mechanical properties. Mater. Sci. Eng A., 2009, 515(1-2):38-42.
[13] Perevertov O, Schafer R. Magnetic properties and magnetic domain structure of grain-oriented Fe-3Si steel under compression. Mater. Res. Express, 2016, 3(9): 195-223.
[14] Xiong X, Hu S, Hu K, et al. Texture and magnetic property evolution of non-oriented Fe-Si steel due to mechanical cutting. J. Magn. Magn. Mater., 2015, 401: 982-990.
[15] Bolfarini C, Silva M C A, Jr A M J, et al. Magnetic properties of spray-formed Fe–6.5%Si and Fe–6.5%Si–1.0%Al after rolling and heat treatment. J. Magn. Magn. Mater., 2008, 320(20): 653–e656.
[16] Mei R B, Bao L, Cai B, et al. Piecewise modeling of flow stress of 7075-t6 aluminum alloy in hot deformation. Mater. Trans., 2016, 57(7): 1147-1155.